CIMAC CONGRESS 25
ZURICH, MAY 19 – 23, 2025

# 2025 | 352

# Power distribution in cruise ship generator sets using different fuels under impact of carbon tax

Controls, Automation, Measurement, Monitoring & Predictive Maintenance


## Guozheng Liu, Harbin Engineering University

Yu Ding, Harbin Engineering University
Congbiao Sui, Harbin Engineering University
Shengping Ma, Harbin Engineering University

## ABSTRACT

Amid increasingly stringent greenhouse gas emission (GHG) restrictions, ambitious carbon reduction targets, and the implementation of carbon tax policies, the cruise shipping industry faces significant challenges. This paper employs a large cruise ship as a benchmark to analyze the impact of carbon tax on power distribution using various fuels, with a particular focus on operational efficiency and cruising speed throughout its voyage. A mathematical model evaluates the ship's economic performance and navigational efficiency under various carbon tax scenarios, employing a mixed-integer nonlinear programming method to optimize energy management and reduce operational costs. The power system of the analyzed cruise ship supports three fossil fuels: very low sulfur fuel oil (VLSFO), marine gas oil (MGO), and liquefied natural gas (LNG). Under non-taxation scenarios, the results reveal that cruise ship speed fluctuates minimally with VLSFO and LNG fuels, while MGO exhibits the most pronounced variations. Under current carbon tax policies, the cruise ship using VLSFO achieves the lowest fuel cost at €298,039.35—approximately €71,730.48 lower than MGO—despite incurring the highest carbon tax of €5,464.70. Additionally, the cruise ship using VLSFO exhibits the poorest energy efficiency operational indicator (EEOI) at $6.30\times10^{-6}$ t·$CO_2$/t·nautical miles, exceeding LNG by $2.23\times10^{-6}$ t·$CO_2$/t·nautical miles. As the carbon tax increases, the cruise ship's total operational costs increase proportionally, while total voyage GHG emissions decline. With VLSFO, for instance, operational costs rise from €451,984.00 to €513,652.05 (a 13.64% increase), while lifecycle GHG emissions decrease from 2,224.45 to 2,191.15 tonnes (a 1.50% reduction). The cruise ship’s EEOI exhibits a notable reduction, from $8.55\times10^{-6}$ to $8.27\times10^{-6}$ t·$CO_2$/t·nautical miles, indicating a 3.15% improvement. This approach offers an effective framework for analyzing cruise ships' operational costs and navigational efficiency under various carbon tax scenarios.

## 1 INTRODUCTION

A typical cruise ship, with a passenger capacity ranging from 100 to 6,000, consumes approximately 250 tons of fuel daily, significantly contributing to global carbon emissions [1]. The International Council on Clean Transportation reports that emissions growth is outpacing efficiency gains, highlighting the pressing need for enhanced carbon control policies [2]. Cap-and-trade systems and carbon taxes are among the most widely adopted strategies, with carbon taxes generally considered more effective in balancing social and economic costs [3]. Nevertheless, implementing a carbon tax introduces challenges due to the intricate economic and market dynamics. In the cruise industry, operating profits are impacted by factors such as shipbuilding costs, fuel prices, and ticket revenues, with the imposition of a carbon tax further elevating fuel costs and significantly reducing profit margins [4]. Consequently, an intricate interplay exists between cruise operational costs and carbon tax policies. Effective carbon control policies must account for these industry-specific factors to achieve emission reductions without impeding the sector's sustainable development.

The introduction of a maritime carbon tax is anticipated to substantially impact the power distribution of ship engines, thereby affecting various aspects of ship operations. Ship operators may need to adjust routes to minimize fuel consumption and reduce exposure to carbon costs. A study by Tsung-Chen Lee et al., using the GTAP-E model, analyzes the implications of a maritime carbon tax policy on freight costs for container ships [5]. Speed optimization is another key strategy to reduce emissions and fuel consumption, although it may extend voyage duration. Research by Yuwei Xing et al. shows that higher carbon taxes and stricter emission caps reduce carbon emissions but also necessitate more container ships to meet demand due to slower speed [6]. Additionally, port call schedules may need to be adjusted more frequently to align with carbon emission policies and mitigate costs. Maxim A. Dulebenets proposes a hybrid mathematical model for green ship scheduling, which integrates carbon dioxide ($CO_2$) emission costs during sailing and at ports. This study suggests that higher carbon expenditures will substantially modify ship scheduling, facilitating more sustainable operations [7]. In response to carbon taxes, ship operators are also likely to adopt cleaner fuels, such as liquefied natural gas (LNG) and methanol, as a cost-saving measure. Research by Murat Bayraktar suggests that switching from heavy fuel oil and marine diesel oil (MGO) to LNG and methanol could reduce operational costs by approximately 31% in scenarios with elevated carbon taxes while also lowering $CO_2$ emissions [8]. Overall, ship operators will need to optimize routes, speed, and fuel choices to manage operational costs and adhere to increasingly stringent carbon regulations, while fostering the long-term sustainability of the maritime industry.

Existing research primarily examines the impact of carbon tax implementation on power distribution in the cruise ship generator sets, with a focus on its impact on operational fuel costs, speed optimization and route selection. However, many studies fail to account for the full lifecycle emissions of marine fuels, which can lead to incomplete or skewed assessments of carbon taxes' impact on operational costs. For example, while some cleaner fuels produce lower emissions during operation, their production and supply chain emissions can exhibit considerably higher levels. A study by the International Maritime Organization, utilizing a lifecycle assessment, reveals that the lifecycle greenhouse gas (GHG) emissions associated with methanol surpass those of certain conventional marine fuels [9]. Similarly, Jinjin Huang et al. apply lifecycle assessment to a very large crude carrier operating between the Middle East and China to analyze the emissions impacts of alternative fuels. Their findings indicate that replacing MGO with fossil-based methanol and ammonia reduces local emissions but fails to achieve a net decrease in total annual GHG emissions over the full well-to-wake lifecycle [10]. Designing effective carbon tax policies necessitates a full-lifecycle emissions approach to fuel evaluation by incorporating upstream emissions to avoid inaccurate assessments.

This study uses the Costa cruise ship as a representative case study to assess the impact of carbon tax policies on power distribution in the cruise ship generator sets with different fuel scenarios. The analysis begins by evaluating the well-to-wake lifecycle carbon emissions of very low sulfur fuel oil (VLSFO), MGO, and LNG to provide a holistic perspective on their environmental implications. A mixed-integer nonlinear programming (MINLP) method is utilized to optimize energy management across the Costa cruise ship's voyage. The study examines total voyage operational costs, cruising speed patterns, and the GHG emissions reduction potential of different fuel options for the cruise ship under various carbon tax scenarios.

## 2 BENCHMARK SHIP AND INPUT DATA

This section provides key details about the cruise ship under study, including the economic and technical specifications of its propulsion system. It also provides an analysis of the GHG emission factors of VLSFO, MGO, LNG, and onshore power supply (OPS) over their full lifecycle. Finally, this section summarizes the pertinent carbon tax policies.

### 2.1 Benchmark ship power system configurations

This study examines the Costa cruise ship, focusing on a typical Mediterranean route characteristic of large Costa vessels. The Costa cruise ship is 289.59 meters long, 35.5 meters wide, and has a draught of 8.20 meters. It operates at a maximum speed of 23 knots and a cruising speed of 21.5 knots, accommodating up to 3,780 passengers. Further technical details are summarized in Table 1.

Table 1. Main particular of Costa cruise ship [11]

| Characteristics | Value | Characteristics | Value |
|---|---|---|---|
| Gross Tonnage (t) | 114.29 | Length Overall (m) | 289.59 |
| Breadth (m) | 35.5 | Draught (m) | 8.20 |
| Max Speed (kn) | 23.0 | Service Speed (kn) | 21.5 |

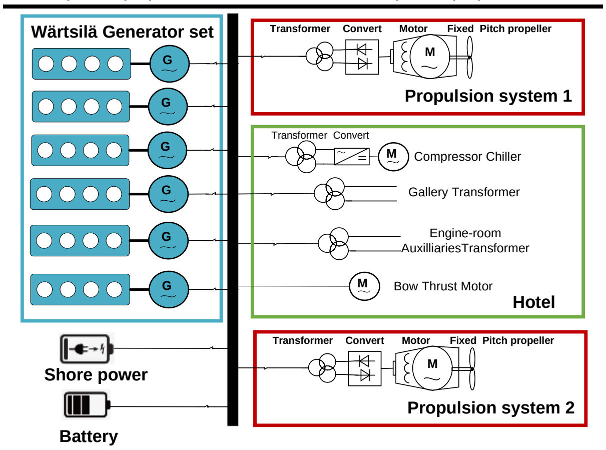


Figure 1. Ship power system configuration [12]

The power system configuration of the Costa cruise ship examined in this research is depicted in Figure 1. The baseline configuration comprises six Wärtsilä 12V46C engines fueled by MGO for electricity generation, alongside two 21 MW propellers for propulsion. To analyze the impact of carbon tax policies on power distribution in the cruise ship generator sets using different fuel scenarios, the power system is reconfigured with alternative engine types and configurations. For example, in the VLSFO fuel scenario, the system employs three Wärtsilä 12V 46F and three Wärtsilä 9L 46F engines. In the LNG fuel scenario, three Wärtsilä 12V 46DF and three Wärtsilä 9L 46DF engines are used to ensure a total capacity equivalent to the original system. To enhance fuel efficiency and further reduce emissions, the VLSFO and MGO configurations integrate selective catalytic reduction (SCR) systems and scrubbers.

### 2.2 Energy demand and techno-economic parameters

The fluctuations in electrical load throughout the voyage, encompassing demands for hospitality, entertainment, auxiliary machinery, and control systems, are depicted in Figure 2. At maximum cruising speed, total power demand peaks at 21,531.54 kW, while the minimum load during port stays is 7,015.92 kW. Besides, Figure 3 illustrates the relationship between cruising speed and propulsion energy demand, with a peak of approximately 35,932.52 kW at 23 knots.

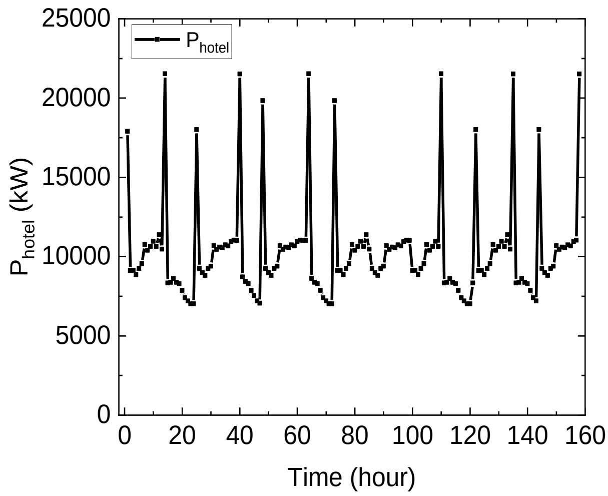


Figure 2. Electrical power hourly distribution [13]

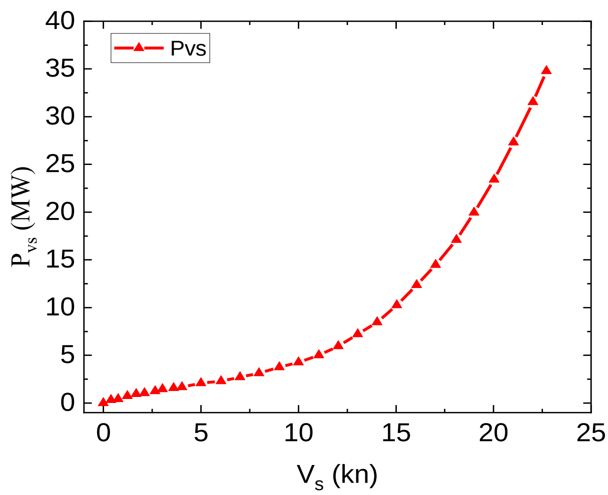


Figure 3. The relationship curve between ship speed and propulsion power [12]

Table 2 outlines the fuel consumption of the engines based on Wärtsilä specifications, while Table 3 summarizes the associated maintenance costs for the power systems. Table 4 provides a comparison of prices and lifecycle GHG emissions for the three fuels assessed in this study—MGO, VLSFO, and LNG—available in the port of Rotterdam. Notably, LNG exhibits marginally higher GHG emissions than MGO, largely due to methane leakage during operations, which amplifies its overall GHG impact. Additionally, Table 4 also presents a range of onshore power supply prices, highlighting cost variations across different ports.

Table 2. Wärtsilä engine specific fuel oil consumption [12, 14, 15]

| Engine type | Fuel type | Specific fuel oil consumption (g, kJ/kWh) | | | |
|---|---|---|---|---|---|
| | | 100% | 85% | 75% | 50% |
| 12V46C | MGO | 200.54 | 196.53 | 196.47 | 209.43 |
| 12V46F | VLSFO | 182.5 | 176.8 | 185.9 | 195 |
| 9L46F | VLSFO | 185.3 | 178.7 | 188.8 | 197.9 |
| 12V46DF | LNG | 7350 | 7485 | 7594 | 8071 |
| 9L46DF | LNG | 7350 | 7485 | 7594 | 8071 |

Table 3. Maintenance cost of different equipment [16]

| Equipment type | Total power (MW, kWh) | Maintenance cost (€/kWh, €/kg $SO_2$ removed) |
|---|---|---|
| Diesel generator set | 75.6 | 0.012 |
| Dual fuel generator set | 72.135 | 0.012 |
| Battery | 4000 | - |
| Scrubber | - | 0.395 |
| SCR | - | 0.006 |

Table 4. Economic and lifecycle emission parameters of fuel and the onshore power supply [17-19]

| Energy type | Energy cost (€/t, €/kWh) | GHG (kg/kg fuel, kg/kWh) | Sulphur content (%) |
|---|---|---|---|
| MGO | 691.31 | 3.76 | 0.15 |
| VLSFO | 523.22 | 3.75 | 0.5 |
| LNG | 654.37 | 4.31 | - |
| Onshore power supply | 0.127-0.539 | 0.3619 | - |

### 2.3 Carbon tax policy

The carbon emission cost refers to the cost incurred through a carbon tax, which allows the emission of 1 ton of $CO_2$ or an equivalent amount of higher-impact GHGs, such as nitrous oxide and methane. These allowances can be obtained, bought, or exchanged in trading markets. The projected carbon tax values for 2030 and 2040 in the European Union are derived from the World Energy Outlook report, with annual estimates calculated through interpolation. Figure 4 illustrates four scenarios, including non-taxation (NT), current policies (CP), stated policies (SP), and sustainable development (SD). The non-taxation scenario assumes no carbon pricing, reflecting the current marine industry situation, while the current policies scenario considers policies implemented by mid-2017. The stated policies scenario is current policies and today's policy intentions and targets. The sustainable development scenario outlines policies to meet the UN's 2030 Sustainable Development Agenda, representing the long-term vision for the energy sector.

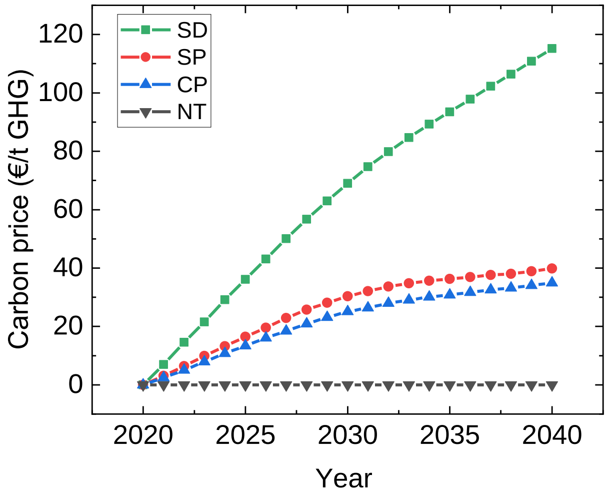


Figure 4. Carbon tax scenarios [20]

## 3 MATHEMATICAL MODEL OF SHIP POWER SYSTEM

This section focuses on developing an optimization model for ship energy management through the MINLP methodology and provides a comprehensive analysis of the objective functions and constraints.

### 3.1 Ship energy management strategy

The ship energy management strategy is designed to optimize onboard equipment operation, considering external load conditions and operational characteristics across various energy sources. This strategy aims at minimizing operational costs while ensuring safety and efficiency. This problem is conventionally modeled as a MINLP problem, as it entails optimizing discrete variables (e.g., equipment start/stop decisions) alongside continuous variables (e.g., equipment output levels). The branch-and-bound method, widely used in MINLP problems, originates from the pioneering work of Land, Doig, and Dakin in the 1960s [21]. The fundamental principles of the branch-and-bound approach are discussed in detail in this section. The overall process flow of the algorithm is depicted in Figure 5. For maximization problems, the algorithm iteratively refines the lower bound (denoted as z) by leveraging it to prune non-optimal nodes. This refinement occurs when the optimal solution to a subproblem is identified, thus improving the objective function value. The optimal solution of a subproblem establishes a lower bound for *z*. Additionally, the algorithm integrates a mechanism to determine the upper bound of the subproblem's objective value.

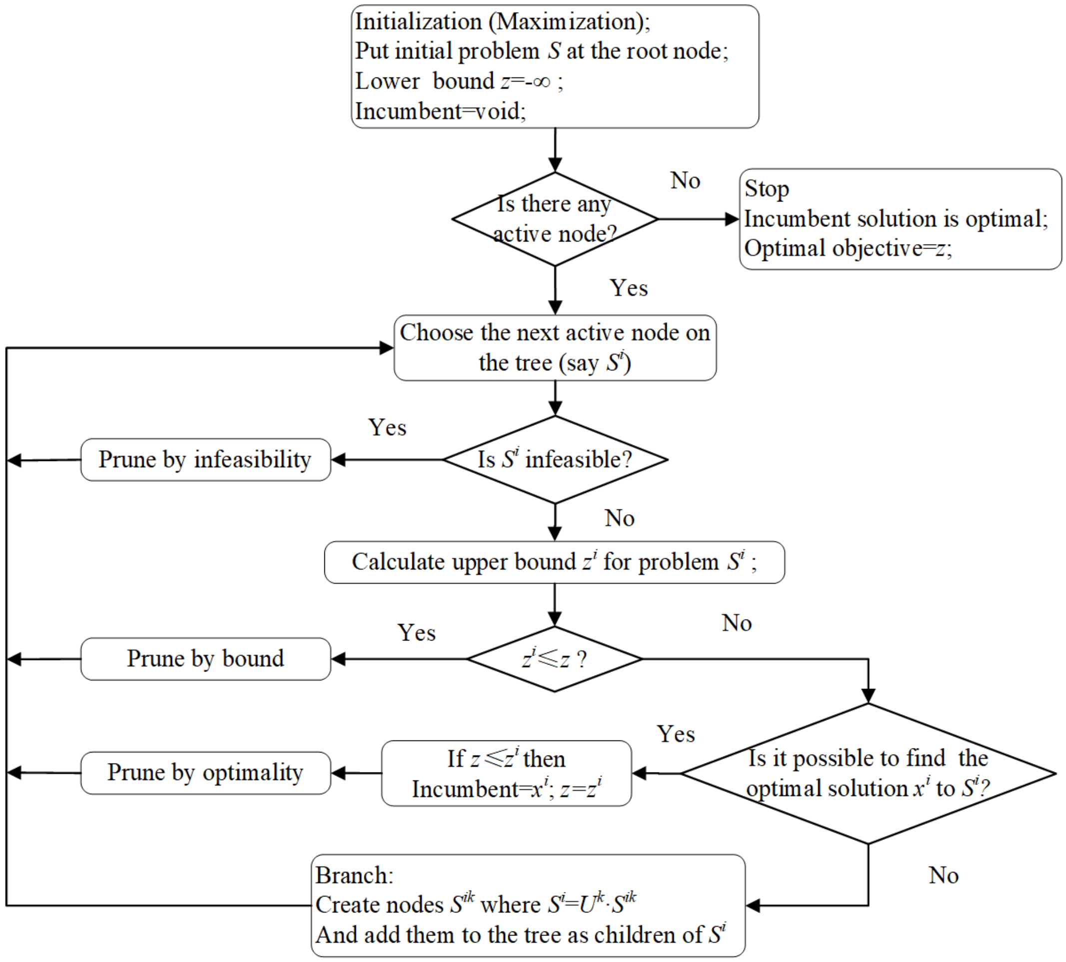


Figure 5. General branch and bound algorithm of MINLP problem [22]

### 3.2 Objective function

The primary optimization objective of this study is to minimize the operational cost $f_{cost}$, as defined by the calculation formula below.

$$f_{\text{cost}} = f_{fuel} + f_{main} + f_{OPS} + f_{tax} + f_{punish} \tag{1}$$

Where:

- $f_{fuel}$ denotes the fuel expenditures for each operational phase of the generator set, expressed in €, with the calculation formula provided below.

$$f_{fuel} = \sum_{t=1}^{158-OPH} \sum_{s} sfc_{t,s} \cdot P_{t,s} \cdot h_t \cdot C_{fuel} \tag{2}$$

Where $t$ denotes the t-th operational phase of a power facility; $OPH$ represents the total operational hours during which the ship is connected to onshore power supply; $s$ represents the s-th generator set; $P_{t,s}$ denotes the power output of the generator set $s$ during phase $t$ in kW; $h_t$ refers to the operational hours of phase $t$; $C_{fuel}$ denotes the price of various fuel types in €/kg; $sfc_{t,s}$ represents the amount of fuel consumed, in kg/kWh, during the t-th operational phase.

The fuel consumption of the generator set can be accurately modeled using segmented linear functions, as illustrated below.

$$sfc_D^n(P_{D,i}(t)) = \alpha_{D,i}^n \cdot P_{D,i}(t) + \beta_{D,i}^n \tag{3}$$

Where $P_{D,i}(t)$ is the power output of the i-th ship's generator set at time $t$ in kW; $\alpha^n_{D,i}$ and $\beta^n_{D,i}$ are the coefficients derived from the fitted linear function.

- $f_{main}$ represents the maintenance cost of each piece of equipment in €, and the corresponding calculation formula is as follows.

$$f_{main} = \sum_{t=1}^{158-OPH} \sum_{s} C_{m,s} \cdot P_{t,s} \cdot h_t \tag{4}$$

Where $C_{m,s}$ denotes the maintenance cost factor of the s-th facility in €/kWh.

- $f_{OPS}$ represents the onshore power supply cost incurred by the ship while docked at port, expressed in €, with the corresponding calculation formula as follows.

$$f_{OPS} = \sum_{t=1}^{OPH} C_{OPS} \cdot P_{OPS,t} \cdot h_t \quad (5)$$

Where $C_{OPS}$ represents the onshore power supply cost factor in €/kWh; $P_{OPS,t}$ denotes the onshore power supply in the t-th operational phase in kW.

- $f_{tax}$ is the cost due to carbon taxation price for the GHG emissions concerning the generator set and onshore power supply in €, the specific calculation formula is as follows.

$$\begin{aligned} f_{tax} = (&\sum_{t=1}^{158-OPH} \sum_{s} sfc_{t,s} \cdot P_{t,s} \cdot h_t \cdot C_{fuelGHG} - E_{fuel} \\ &+ \sum_{t=1}^{OPH} P_{OPS,t} \cdot h_t \cdot C_{OPSGHG} - E_{OPS}) \cdot C_{tax} \end{aligned} \quad (6)$$

Where $C_{tax}$ denotes the GHG emissions carbon tax in €/ kg. $C_{fuelGHG}$ denotes the GHG emissions factor of marine fuels in kg·GHG/kg·fuel. $C_{OPSGHG}$ denotes the GHG emissions factor of onshore power supply in kg·GHG/kWh. $E_{fuel}$ and $E_{OPS}$ represent 80.75% of the GHG emissions from fuel use and onshore power supply, respectively, throughout the entire voyage of the cruise ship under the non-taxation scenario [23].

- $f_{punish}$ represents the start-stop constraints for the generator set, designed to avoid frequent switching on and off of the equipment.

$$f_{punish} = \sum_{t=1}^{158-OPH} \sum_{s} (P_{t+1,s} - P_{t,s}) \cdot C_{punish} \quad (7)$$

Where $C_{punish}$ is the penalty coefficient for the start-stop operations of the generator set, set at €1000.

### 3.3 System constraints

The optimization constraints in this study are divided into two main categories: energy balance constraints and equipment output constraints. The energy balance constraints primarily address the electrical energy equilibrium within the system.

(1). Electricity balance constraints

The electrical load of the ship is managed by six generator sets, and the following equation governs the electrical balance.

$$\begin{aligned} &\sum_{i=1}^{6} P_{D,i}(t) \cdot X_{D,i}(t) \cdot \eta_{gen} + P_{OPS}(t) \cdot X_{OPS}(t) \\ &= P_{vs}(t) + P_{hotel}(t) + P_{Bat}(t) \end{aligned} \quad (8)$$

Where $X_{D,i}(t)$ represents the operational status (on/off) of the i-th generator set at time $t$; $\eta_{gen}$ indicates the operational efficiencies of the generator, typically set at 0.97; $P_{OPS,i}(t)$ denotes the power output of the onshore power supply at time $t$ in kW; $X_{OPS,i}(t)$ represents the operational status (on/off) of onshore power supply at time $t$; $P_{hotel}(t)$ indicates the electrical load required by the ship's hotel services at time $t$ in kW; $P_{Bat}(t)$ denotes the battery power output at time $t$ in kW; $P_{vs}(t)$ indicates the electrical load required for the ship's navigation systems at time $t$ in kW.

The relationship between the propulsion load and ship speed is provided, as follows:

$$P_{vs}(t) = c_1 v(t)^2 + c_2 v(t) + c_3 \quad (9)$$

Where $v(t)$ represents the ship's speed at time t in kn; $c_1$, $c_2$ and $c_3$ are coefficients related to the ship's speed.

This equation is crucial for optimal power management, as it reflects the relationship between the cruise ship's propulsion load and cruising speed. By adjusting the cruising speed, the propulsion power demand can be optimized, with different speed corresponding to varying power requirements.

(2). Generator set power constraints

The output power of the generator set is constrained within a range typically between 25% and 90% of its nominal capacity [24].

$$P_D^{\min} \le P_{D,i}(t) \le P_D^{\max} \quad (10)$$

(3). Battery energy constraints

The energy constraints on the battery primarily limit its discharge and charge capacities. To prolong battery life, the state of charge ($SOC$) must be maintained within a specified range (0.25–0.85 in this study) [25], as follows：

$$\begin{aligned} &SOC_{\min} \le SOC(t) = \frac{E_{ESS}(t)}{E_{ESS}} \le SOC_{\max} \\ &E_{ESS}(t) = \begin{cases} E_{ESS}(t-1) + \dfrac{P_{ESS}(t)}{\eta_{dc}} \cdot \Delta t, & P_{ESS}(t) \le 0 \\ E_{ESS}(t-1) + P_{ESS}(t) \cdot \eta_{ch} \cdot \Delta t, & P_{ESS}(t) \ge 0 \end{cases} \\ &\sum_{t=1}^{158} P_{ESS}(t) = 0 \end{aligned} \quad (11)$$

Where $E_{ESS}(t)$ denotes the battery capacity at time $t$ in kWh; $P_{ESS}(t)$ represents the battery power at time $t$ in kW; $\eta_{ch}$ and $\eta_{dc}$ indicate the charging and discharging efficiencies of the battery, respectively, which is set at 0.97 [26]; $\Delta t$ refers to the charging or discharging duration, in hours.

(4). Voyage distance constraint

$$\begin{aligned} & Dis(t) = Dis(t-1) + v(t)\cdot\Delta t \\ & \sum_t v(t)\cdot\Delta t \geq Dis_{i\rightarrow j} \end{aligned} \qquad (12)$$

Where $Dis(t)$ represents the distance covered by the cruise ship at time $t$ in the nautical mile; $Dis_{i\rightarrow j}$ refers to the distance between location $i$ and location $j$ in the nautical mile.

(5). Speed constraint

$$\begin{aligned} & 0 \leq v_{dep}(t), v_{app}(t) \leq 4\ (kn) \\ & 4 \leq v_{cru}(t) \leq 23\ (kn) \end{aligned} \qquad (13)$$

Where $v_{dep}(t)$ and $v_{app}(t)$ represent the cruise ship's speed during departure and approach to the port, respectively; $v_{cru}(t)$ refers to the ship's cruising speed during normal operations when it is sailing between ports.

## 4 RESULTS

The results section details the distribution of power and variations in cruising speed of the cruise ship across various fuels in the non-taxation scenario. Subsequently, the analysis focuses on changes in operational costs under current policies for different fuel types. Finally, the study investigates trends in operational costs and the Energy Efficiency Operational Indicator (EEOI) as the carbon tax increases across each fuel type.

### 4.1 Power distribution of the cruise ship using different fuels

The distribution of power between the generator and battery systems when the cruise ship operates on MGO, VLSFO, and LNG fuels are shown in Figure 6 to Figure 8 respectively. The battery stabilizes generator output, enabling the engine to operate with improved efficiency. Additionally, the figures highlight that the battery predominantly charges during the voyage and discharges when docked to meet the cruise ship's electrical requirements. Nevertheless, the battery's charging and discharging patterns exhibit significant variations across different fuel conditions. For instance, Figure 6 shows that, between hours 111 and 121, the battery charge level is significantly higher under MGO fuel compared to the other two fuel conditions. This behavior is attributed to the higher cost of MGO fuel relative to the other two fuels, coupled with lower onshore power supply prices during this period, rendering onshore power supply more cost-effective than MGO-based generation.

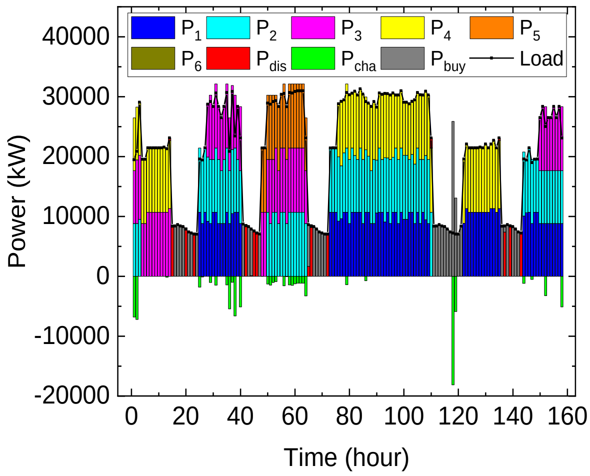


Figure 6. Power distribution of the cruise ship using MGO fuel

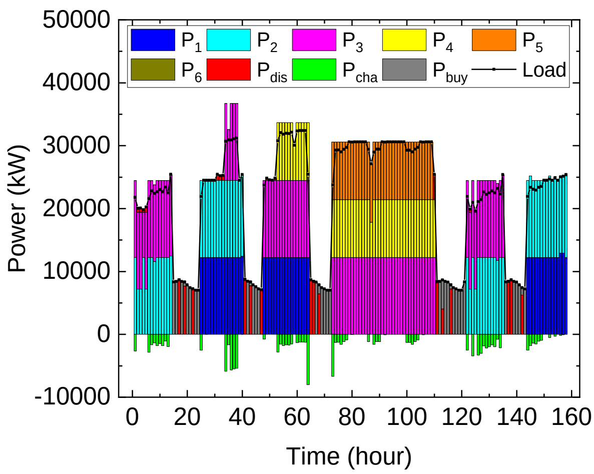


Figure 7. Power distribution of the cruise ship using VLSFO fuel

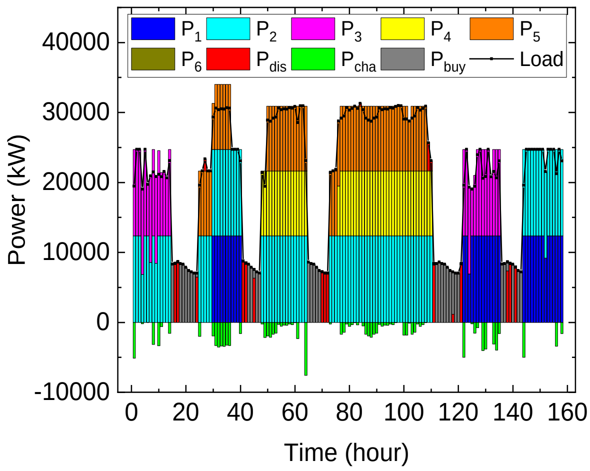


Figure 8. Power distribution of the cruise ship using LNG fuel

The cruising speed and voyage performance of the cruise ship under a non-taxation scenario when using MGO, VLSFO, and LNG fuels are illustrated in Figure 9. Minimal speed variations are observed with LNG and VLSFO fuels, whereas MGO fuel demonstrates more significant speed fluctuations. This discrepancy arises from the generator configurations: the MGO system utilizes a single-specification generator, while the VLSFO and LNG systems incorporate one high-power generator alongside three low-power generators, offering greater flexibility in power adjustments and resulting in more stable output.

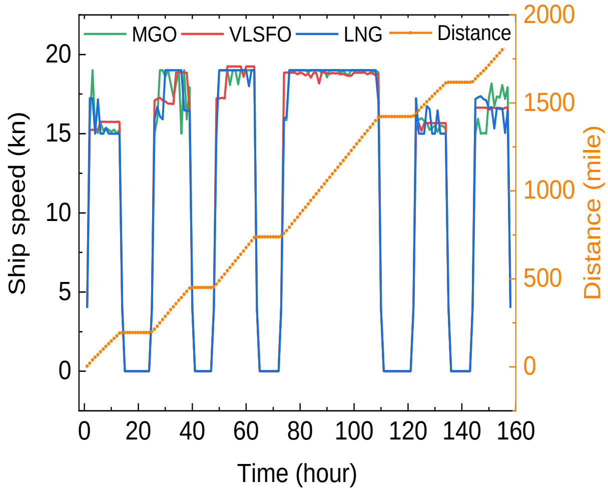


Figure 9. Cruise ship voyage using different fuels under the non-taxation scenario

## 4.2 Impact of different fuels on cruise ship speed and operational costs under current policies

This section analyzes cruising speed and operational cost variations of the cruise ship under current policies using MGO, VLSFO, and LNG fuels. Figure 4 highlights government projections for a carbon tax of 13.41 €/ t GHG by 2025. Figure 10 illustrates variations in cruising speed across the three fuels after the implementation of the carbon tax policy. Compared to Figure 9, the carbon tax policy results in greater speed fluctuations, particularly for MGO fuel. The introduction of the carbon tax notably amplifies battery charge-discharge cycles, especially around port entry and exit, further intensifying speed variability.

Figure 11 depicts the battery's charge-discharge patterns under different fuel conditions. The figure indicates that the battery's charge-discharge state is largely comparable when using VLSFO and LNG fuels. However, with MGO fuel, the charge-discharge state exhibits abnormal behavior. Notably, when the ship operates on MGO fuel between hours 65 and 110, the battery's SOC remains relatively stable, indicating that the MGO generator operates within a high-efficiency range during this period.

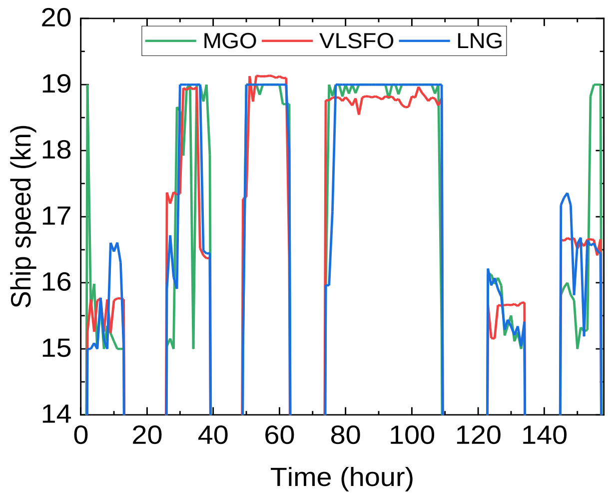


Figure 10. Cruise ship speed with different fuels under the current policies

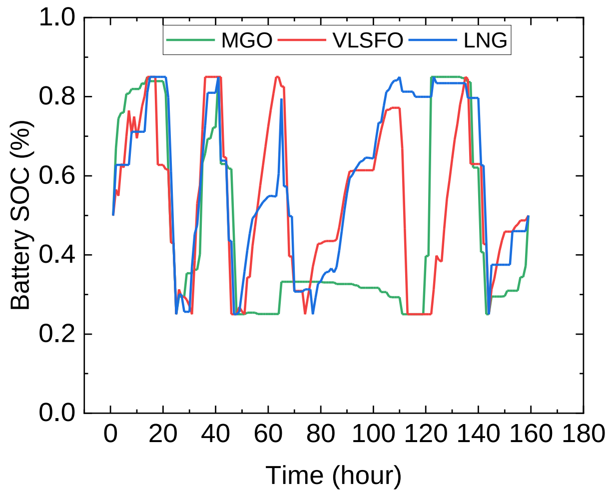


Figure 11. Battery SOC with different fuels under the current policies

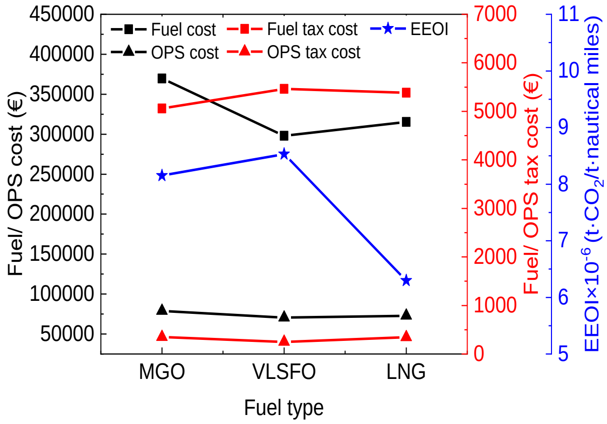


Figure 12. Fuel and onshore power supply costs, as well as the EEOI, for the cruise ship using different fuels under the current policies

The fuel and onshore power supply costs, as well as the EEOI values across various fuel conditions, are depicted in Figure 12. The data suggest that onshore power supply costs and associated carbon taxes remain largely consistent across fuel types. The fuel cost is highest with MGO at €369,769.83, surpassing VLSFO fuel costs by €71,730.48. However, VLSFO incurs the highest carbon tax cost at €5,464.70, exceeding MGO's carbon tax cost by €404.94. In contrast, the LNG-fueled generator exhibits the lowest EEOI at 6.297 × $10^{-6}$ t·$CO_2$/t·nautical mile, approximately 35.47% lower than VLSFO's highest EEOI, underscoring LNG's advantage in minimizing $CO_2$ emissions during operation.

### 4.3 Impact of carbon tax policy on cruise ship speed and operational costs

Figure 13 illustrates the variations in cruising speed under different carbon tax policies for VLSFO fuel. As the carbon tax increases, speed fluctuations progressively decrease. At a €150/ton GHG carbon tax, the maximum cruising speed reaches 19.63 knots, which is 0.38 knots higher than in the non-taxation scenario. In high-carbon-tax scenarios, the ship prioritizes onshore power supply charging, enabling the generator to operate more efficiently and deliver greater output for direct propulsion at sea. Figure 14 illustrates the SOC of the battery with VLSFO generators under varying carbon tax policies. The data reveal that between hours 65 and 72, the battery continues charging under the €150/ton GHG carbon tax policy, whereas it discharges under the other two policies. This behavior occurs because, at higher carbon tax levels, onshore power supply becomes more cost-effective than generator-based power.

Figure 15 depicts variations in GHG emissions from the cruise ship and onshore power supply under different carbon tax policies. The results demonstrate that higher carbon taxes significantly reduce the ship's GHG emissions, particularly for VLSFO, where emissions decline from 2139.60 tons to 2072.16 tons. By contrast, MGO exhibits a modest reduction of 34.54 tons. Furthermore, increasing carbon taxes result in gradual rises in onshore power supply emissions, with VLSFO and LNG exhibiting the most significant changes. In the non-taxation scenario, VLSFO yields the lowest onshore power supply emissions at 84.86 tons, whereas under the maximum carbon tax, LNG achieves the lowest emissions at 116.46 tons, approximately 2.53 tons lower than VLSFO. MGO produces the highest onshore power supply emissions, increasing from 103.50 tons to 121.79 tons. However, the total GHG emissions from both the fuel and onshore power supply sources will decrease. For instance, with VLSFO, the overall lifecycle carbon emissions decrease from 2,224.45 tons to 2,191.15 tons, reflecting a reduction of 1.50%.

Figure 16 illustrates the operational costs associated with MGO, VLSFO, and LNG fuels under various carbon tax policies, covering maintenance, generator startup/shutdown, fuel, onshore power supply, and carbon tax costs. The results indicate that as the carbon tax increases, maintenance and startup costs remain stable, fuel costs gradually decrease, while onshore power supply, fuel carbon tax, and onshore power supply carbon tax costs increase. Across all carbon tax policies, fuel costs consistently constitute the largest proportion, followed by onshore power supply and maintenance costs. Under a €75/ton GHG carbon tax policy, fuel carbon tax costs exceed generator startup/shutdown costs; in a €150/ton GHG carbon tax policy scenario, fuel carbon tax costs for MGO and VLSFO are comparable to maintenance costs, while LNG's fuel carbon tax costs approach those of LNG generator maintenance.

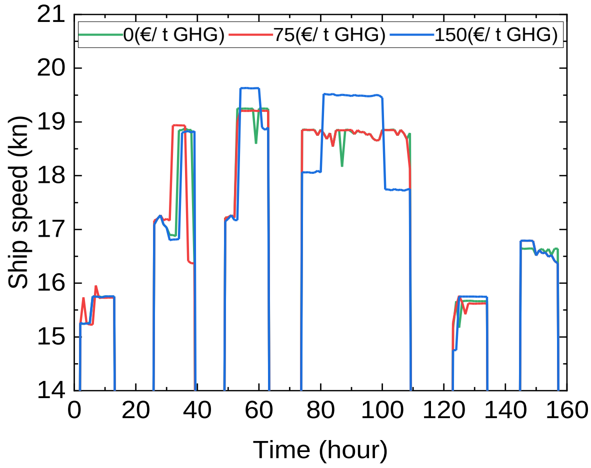


Figure 13. Cruise ship speed using VLSFO generators under different carbon tax policies

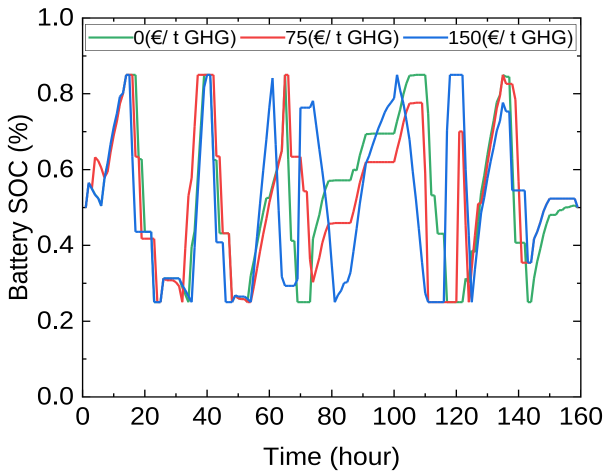


Figure 14. Battery SOC using VLSFO generators under different carbon tax policies

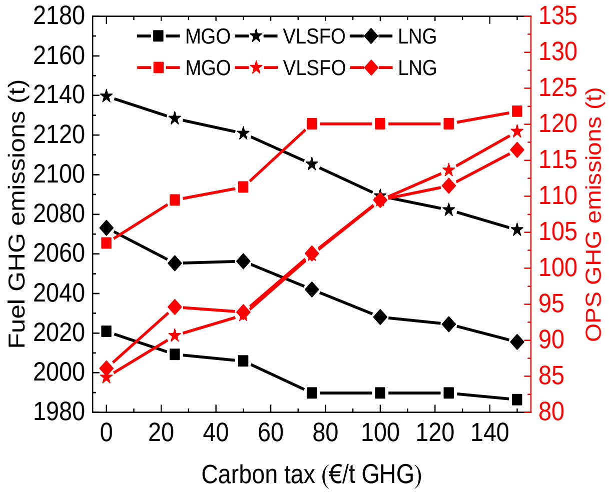


Figure 15. GHG emission variation curves of cruise ship and onshore power supply under different carbon tax policies

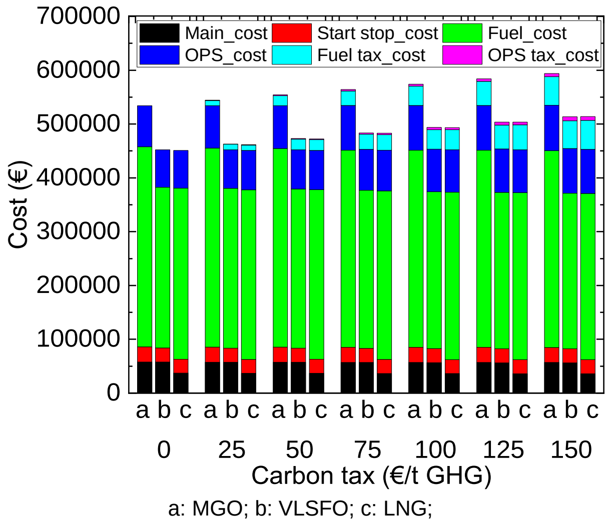


Figure 16. Operational costs of the cruise ship under various carbon tax policies

Table 5 provides a summary of the total operational costs for the cruise ship with MGO, VLSFO, and LNG fuels under different carbon tax policies. The data indicate that across different carbon tax policies, the total cost is consistently highest for MGO fuel, rising from €534,175.47 to €593,763.19, an increase of 11.15%. However, under a carbon tax policy ranging from €0 to €125/ton GHG, the cruise ship using LNG fuel incurs the lowest operational cost. At €150/ton GHG, VLSFO achieves the lowest cost, amounting to €513,652.05 and resulting in a savings of approximately €410 compared to LNG. This is because, over its lifecycle, the GHG conversion factor for VLSFO is lower than that of LNG.

Table 6 presents the EEOI for the cruise ship using MGO, VLSFO, and LNG fuels under different carbon tax policies. The data indicate that increasing the carbon tax significantly reduces the ship's EEOI, contributing to lower $CO_2$ emissions during operation. Among the three fuels, MGO exhibits the highest EEOI value, while LNG has the lowest. VLSFO experiences the most significant impact from the carbon tax, as its EEOI decreases from $8.55 \times 10^{-6}$ to $8.28 \times 10^{-6}$ t·$CO_2$/t·nautical mile, a 3.15% reduction.

Table 5. Total costs of the cruise ship under various carbon tax policies

| Carbon tax (€/t GHG) | Ship MGO cost (K€) | Ship VLSFO cost (K€) | Ship LNG cost (K€) |
|---|---|---|---|
| 0 | 534175.47 | 451984.00 | 450876.89 |
| 25 | 544244.61 | 462890.13 | 461649.37 |
| 50 | 554290.97 | 473165.78 | 472308.95 |
| 75 | 564207.34 | 483580.63 | 482934.99 |
| 100 | 574046.82 | 493532.51 | 493396.70 |
| 125 | 583912.46 | 503744.48 | 503712.75 |
| 150 | 593763.19 | 513652.05 | 514060.12 |

Table 6. EEOI of the cruise ship under various carbon tax policies

| Carbon tax (€/t GHG) | Ship MGO EEOI ($\times 10^{-6}$ t·$CO_2$/t· nautical miles) | Ship VLSFO EEOI ($\times 10^{-6}$ t·$CO_2$/t· nautical miles) | Ship LNG EEOI ($\times 10^{-6}$ t·$CO_2$/t· nautical miles) |
|---|---|---|---|
| 0 | 8.20 | 8.55 | 6.35 |
| 25 | 8.15 | 8.50 | 6.29 |
| 50 | 8.14 | 8.47 | 6.30 |
| 75 | 8.07 | 8.41 | 6.25 |
| 100 | 8.07 | 8.35 | 6.21 |
| 125 | 8.07 | 8.32 | 6.20 |
| 150 | 8.06 | 8.28 | 6.17 |

## 5 CONCLUSIONS

This study employs a MINLP methodology to optimize energy management throughout the cruise ship's voyage, aiming to minimize the operational costs.

(1). In the non-taxation scenario, the generator operates efficiently with MGO, VLSFO, and LNG fuels, while the battery predominantly charges during sea operations. Under these conditions, the cruise ship experiences minimal speed fluctuations, enabling smoother operations with VLSFO and LNG fuels.

(2). Under current policies, cruising speed fluctuations increase significantly, especially when using MGO fuel. Moreover, under current policies, the cruise ship using VLSFO achieves the lowest fuel cost at €298,039.35, which is approximately €71,730.48 lower than MGO fuel, despite incurring the highest carbon tax of €5,464.70. Additionally, VLSFO records the highest EEOI at $6.3 \times 10^{-6}$

t·$CO_2$/t·nautical mile, which is 2.23 × $10^{-6}$ t·$CO_2$/t·nautical mile higher than LNG.

(3). As carbon tax levels rise, the cruise ship's total operational costs progressively increase, while carbon emissions decline. For instance, with VLSFO, operational costs increase from €451,984.00 to €513,652.05, reflecting a 13.64% rise, while lifecycle carbon emissions decrease from 2,224.45 tons to 2,191.15 tons, representing a 1.50% reduction. Simultaneously, the EEOI decreases from 8.55 × $10^{-6}$ to 8.27 × $10^{-6}$ t·$CO_2$/t·nautical mile, indicating improved energy efficiency.

## 6 DEFINITIONS, ACRONYMS, ABBREVIATIONS

| | |
|---|---|
| **$CO_2$:** | Carbon dioxide |
| **CP:** | Current policies |
| **EEOI:** | Energy efficiency operational indicator |
| **GHG:** | Greenhouse gas |
| **LNG:** | Liquefied natural gas |
| **MGO:** | Marine gas oil |
| **MINLP:** | Mixed-integer nonlinear programming |
| **NT:** | Non-taxation policies |
| **OPH:** | Total operational hour in port |
| **OPS:** | Onshore power supply |
| **SD:** | Sustainable development |
| **SCR:** | Selective catalytic reduction |
| **SOC:** | State of charge |
| **SP:** | Stated policies |
| **VLSFO:** | Very low sulfur fuel oil |
| $C_{fuel}$: | Fuel price |
| $C_{OPS}$: | Onshore power supply cost factor |
| $C_{m,s}$: | Maintenance cost factor of the s-th facility |
| $C_{punish}$: | Penalty factor for the start-stop operations of the generator set |
| $C_{tax}$: | GHG emissions factor |
| $Dis$: | Distance covered by the cruise ship |
| $Dis_{i\to j}$: | Distance between location *i* and location *j* in nautical mile |
| $E_{ESS}$: | Battery capacity |
| $f_{cost}$: | Operational cost of ship |
| $f_{fuel}$: | Operational fuel cost of ship |
| $f_{main}$: | Maintenance cost of each equipment |
| $f_{punish}$: | Start-stop constraints for the generator set |
| $f_{OPS}$: | Onshore power supply cost of ship |
| $f_{tax}$: | Carbon taxation price cost of ship |
| $h_t$: | Operational hours of phase *t* |
| $P_{Bat}$: | Battery power output |
| $P_D$: | Power output of the ship's generator set |
| $P_{ESS}$: | Battery power |
| $P_{OPS,t}$: | Onshore power supply in the t-th operational phase |
| $P_{hotel}$: | Electrical load required by the ship's hotel services |
| $P_{OPS,t}$: | Power output of the onshore power supply in the t-th operational phase |
| $P_{t,s}$: | Power output of the generator set *s* |
| $P_{VS}$: | Electrical load required for the ship's navigation systems |
| $sfc_{t,s}$: | Amount of fuel consumed |
| $v$: | Ship's speed |
| $v_{app}$: | Cruise ship's speed approach to the port |
| $v_{cru}$: | Ship's cruising speed during normal operations |
| $v_{dep}$: | Cruise ship's speed departure to the port |
| $X_{D,i}$: | Operational status of the i-th generator set |
| $X_{OPS,i}$: | Operational status of onshore power supply |
| $\eta_{ch}$: | Charging efficiencies of the battery |
| $\eta_{dc}$: | Discharging efficiencies of the battery |
| $\eta_{gen}$: | Generator efficiencies |
| $\Delta t$: | Charging or discharging duration |

## 7 REFERENCES AND BIBLIOGRAPHY


[1] Ma, H. 2024(accessed 22 October 2024). Cruise Ship Fuel Consumption – All the Details, https://www.cruisehive.com/Cruise-Ship-Fuel-Consumption/105309.

[2] Wang, J and Zhu, W. 2023. Analyzing the development of competition and cooperation among ocean carriers considering the impact of carbon tax policy, *Transportation Research Part E: Logistics and Transportation Review*, 175: 103157.

[3] Wittneben, B B F. 2009. Exxon is right: Let us re-examine our choice for a cap-and-trade system over a carbon tax, *Energy Policy*, 37(6): 2462-2464.

[4] Ros Chaos, S. Pallis, A A. Saurí Marchán, S. Pino Roca, D and Sánchez-Arcilla Conejo, A. 2021. Economies of scale in cruise shipping, *Maritime Economics & Logistics*, 23(4): 674-696.

[5] Lee, T. Chang, Y and Lee, P T W. 2013. Economy-wide impact analysis of a carbon tax on international container shipping, *Transportation Research Part A: Policy and Practice*, 58: 87-102.

[6] Xing, Y. Yang, H. Ma, X and Zhang, Y. 2019. Optimization of ship speed and fleet deployment under

carbon emissions policies for container shipping, *Transport*, 34(3): 260-274.
[7] Dulebenets, M A. 2018. Green vessel scheduling in liner shipping: Modeling carbon dioxide emission costs in sea and at ports of call, *International Journal of Transportation Science and Technology*, 7(1): 26-44.
[8] Bayraktar, M. 2023. Investigation of alternative fuelled marine diesel engines and waste heat recovery system utilization on the oil tanker for upcoming regulations and carbon tax, *Ocean Engineering*, 287: 115831.
[9] Perčić, M. Vladimir, N and Fan, A. 2020. Life-cycle cost assessment of alternative marine fuels to reduce the carbon footprint in short-sea shipping: A case study of Croatia, *Applied Energy*, 279: 115848.
[10] Huang, J. Fan, H. Xu, X and Liu, Z. 2022. Life cycle greenhouse gas emission assessment for using alternative marine fuels: A very large crude carrier (VLCC) case study, *Journal of Marine Science and Engineering*, 10(12): 1969.
[11] Scheepvaartwest. 2024(accessed 22 October 2024). Costa Pacifica - IMO 9378498, https://www.scheepvaartwest.be/CMS/index.php/passengerscruise/4810-costa-pacifica-imo-9378498?highlight=WyJjb3N0YSIsImNyb2NpZXJlIl0=.
[12] Gualeni, P. Boveri, A. Silvestro, F and Margarita, A. 2016. Decision support system for power generation management for an 110000+ GRT cruise ship, *International Journal of Maritime Engineering*, 158(A3).
[13] Dotto, A and Satta, F. 2023. Techno-economic optimization of hybrid-electric power plants onboard cruise ships, *Energy Conversion and Management: X*, 20: 100436.
[14] Wärtsilä. 2020. Wärtsilä 46F product guide.
[15] Wärtsilä. 2020. Wärtsilä 46DF product guide.
[16] Bolbot, V. Trivyza, N L. Theotokatos, G. Boulougouris, E. Rentizelas, A and Vassalos, D. 2020. Cruise ships power plant optimisation and comparative analysis, *Energy*, 196: 117061.
[17] Bunker, S. 2024(accessed 22 October 2024). Rotterdam Bunker Prices, https://shipandbunker.com/prices/am/namatl/us-nyc-new-york.
[18] Valev, N. 2024(accessed 28 June 2024). Electricity prices, https://zh.globalpetrolprices.com/electricity_prices/.
[19] Zincir, B A and Arslanoglu, Y. 2024. Comparative Life Cycle Assessment of Alternative Marine Fuels, *Fuel*, 358: 129995.
[20] Trivyza, N L. Rentizelas, A and Theotokatos, G. 2019. Impact of carbon pricing on the cruise ship energy systems optimal configuration, *Energy*, 175: 952-966.
[21] Leyffer, S. 1998. Integrating SQP and Branch and Bound for Mixed Integer Noninear Programming, *Computational Optimization and Applications*, 18(3): 295-309.
[22] Kianfar, K. 2010. Branch-and-Bound-Algorithms, *Wiley encyclopedia of operations research and management science*.
[23] Yuan, Y. Wang, X. Tong, L. Yang, R and Shen, B. 2023. Research on Multi-Objective Energy Efficiency Optimization Method of Ships Considering Carbon Tax, *Journal of Marine Science and Engineering*, 11(1): 82.
[24] Wang, H and Yun, Q. 2023. Research on Speed Optimization and Adjusting Strategy of Variable Speed Diesel Generator Base on Sliding Interval, *Journal of Marine Science and Engineering*, 11(9): 1682.
[25] Wang, X. Shipurkar, U. Haseltalab, A. Polinder, H. Claeys, F and Negenborn, R R. 2021. Sizing and Control of a Hybrid Ship Propulsion System Using Multi-Objective Double-Layer Optimization, *IEEE access*, 9: 72587-72601.
[26] Hein, K. Xu, Y. Wilson, G and Gupta, A K. 2021. Coordinated Optimal Voyage Planning and Energy Management of All-Electric Ship with Hybrid Energy Storage System, *IEEE Transactions on Power Systems*, 36(3): 2355-2365.